

SUPPORTING INFORMATION APPENDIX

Table S1. Additional aqueous fluid compositions and stable and radioisotope values in mixing zones at the Piccard vent field.

Vent (Year)	Sample ^a	Na (mm)	Cl (mm)	K (mm)	SiO ₂ (mm)	Li (μ m)	Rb (μ m)	Br (mm)	Sr (μ m)	⁸⁷ Sr/ ⁸⁶ Sr	Σ NH ₄ (μ m)	CH ₃ SH (nM)	δ^{13} C _{CO2} (‰)
Beebe Endmember ^b		314	349	11.4	20.0	421	5.59	0.61	21.9	0.7046	36 ^c	11.9 ^c	–
Hot Chimlet 1 (2012)	J2-619-IGT6	418	484	10.3	5.80	141	2.61	0.79	54.4	–	14.2	1760 ^c	-4.3 ^a
	J2-619-IGT3	411	471	10.4	6.37	154	2.71	0.77	51.8	0.70855	16.9	1760 ^c	-4.2 ^d
Hot Chimlet 1 (2013)	N59-IGT6	429	498	10.4	2.81	96.6	1.94	0.78	72.1	–	9.48	–	–
	N59-IGT4	454	530	10.3	0.83	42.8	1.32	0.81	77.4	–	2.58	–	–
Hot Chimlet 3 (2013)	N62-IGT8	445	520	10.4	1.83	66.0	1.64	0.81	76.8	–	8.15	–	–
	N62-IGT7	408	472	10.6	2.60	150	2.40	0.75	65.6	–	15.9	–	–
Hot Chimlet 2 (2012)	J2-620-IGT4	445	511	10.2	2.36	66.1	1.81	0.86	76.4	–	6.17	430 ^c	-4.6
	J2-620-IGT8	451	526	10.4	1.68	51.9	1.64	0.89	81.6	–	2.48	292 ^c	-5.7
Shrimp Gulley 1 (2012)	J2-620-IGT1	438	510	10.2	3.33	86.7	2.03	0.79	74.9	0.70894	7.73	144 ^c	-4.0
	J2-620-IGT2	443	511	10.3	2.94	77.2	1.94	0.81	77.9	–	3.39	83.4 ^c	-4.2
Shrimp Gulley 3 (2013)	N63-IGT6	446	519	10.5	1.93	64.2	1.61	0.81	77.8	–	9.62	–	–
Shrimp Gulley 2 (2012)	J2-618-IGT1	455	528	10.3	1.52	46.6	1.57	0.80	83.7	–	2.94	50.4 ^c	-5.1
	J2-618-IGT3	459	522	10.3	1.46	46.8	1.58	0.76	83.6	–	0.53	44.0 ^c	-5.6
Bottom Seawater		462	540	10.4	0.06	26.5	1.24	0.82	88.5	0.7092	0.10	0.00 ^c	–

^aJason (J2) or Nereus (N##) dive number and isobaric gas-tight sampler number (-IGT).

^bAverage high-temperature vent endmember (For Beebe 1, 3, 5, and Beebe Woods; McDermott et al., 2018.) See McDermott et al. (2018) for IGT data from high temperature fluid samples.

^cData from Reeves et al. (2014). Σ NH₄ and CH₃SH Beebe Endmember reflects the average of two similar measurements for each species.

^dRadiocarbon Δ^{14} C measurement on Σ CO₂ is: Measured Fm = 0.1501 \pm 0.0014, Corrected Fm = -0.0059 \pm 0.0131 (J2-619-IGT6, #OS-105947); Measured Fm = 0.1336 \pm 0.0010, Corrected Fm = 0.0018 \pm 0.0110 (J2-619-IGT3, #OS-104376).

Table S2. Additional aqueous fluid compositions in mixing zones at the Piccard vent field.

Vent (Year)	Sample ^a	Al (μm)	Mn (μm)	Zn (μm)	Cu (μm)	Pb (μm)	Cd (nm)	Ag (nm)	Co (μm)
Hot Chimlet 1 (2012)	J2-619-IGT6	5.0	244	1.40	15.3	0.13	3.5	59	0.28
	J2-619-IGT3	3.8	270	0.047	0.38	<0.080	<1.0	<1.0	<0.002
Hot Chimlet 1 (2013)	N59-IGT6	3.5	125	12.4	9.01	0.40	4.5	<1.0	0.051
	N59-IGT4	2.1	31.0	4.85	8.67	0.53	3.0	<1.0	0.018
Hot Chimlet 3 (2013)	N62-IGT8	<0.010	75	4.02	8.08	0.78	7.3	<1.0	<0.002
	N62-IGT7	1.4	199	6.19	6.09	0.27	5.2	<1.0	0.03
Hot Chimlet 2 (2012)	J2-620-IGT4	3.8	96.9	2.37	21.9	0.21	4.6	97	0.10
	J2-620-IGT8	4.3	66.0	2.45	14.0	0.097	3.0	46	0.17
Shrimp Gulley 1 (2012)	J2-620-IGT1	8.4	114	5.17	21.4	0.31	7.5	102	0.19
	J2-620-IGT2	1.9	90.9	5.29	208	0.12	9.7	38	2.9
Shrimp Gulley 3 (2013)	N63-IGT6	0.17	77.7	18.1	76.2	1.5	13	<1.0	0.051
Shrimp Gulley 2 (2012)	J2-618-IGT1	1.3	44.7	1.31	7.77	<0.080	1.3	22	0.12
	J2-618-IGT3	4.7	43.9	6.31	39.8	0.49	11	56	<0.002
Bottom Seawater		0	0	0	0	0	0	0	0

^aJason (J2) or Nereus (N##) dive number and isobaric gas-tight sampler number (-IGT).

Calculation of positive and negative deviations from theoretical conservative mixtures

A conservative mixing line between the seawater value and the Beebe endmember composition was drawn for Mg^{2+} and select species plotted in Fig. 1. The measured dissolved Mg^{2+} for each mixed fluid was input into this linear regression to solve for a ‘calculated conservative mixture’ composition (Table S3). The difference between the actual measured mixed fluid composition and this theoretical composition is tabulated in Table S3 as either a negative value, when a species has been lost during mixing, or as a positive value, when a species has been gained during mixing.

Table S3. Calculated positive and negative deviations from theoretical conservative mixtures of select aqueous species.

Vent (Year)	Sample ^a	Assessment of Conservative or Non-Conservative Behavior with Mixing	H ₂ (mm)	CH ₄ (mm)	SO ₄ (mm)	ΣH ₂ S (mm)	Fe (mm)	Ca (mm)
Hot Chimlet 1 (2012)	J2-619-IGT6	Calculated Conservative Mixture	6.32	0.0394	18.9	3.81	2.14	9.14
Hot Chimlet 1 (2012)	J2-619-IGT6	Observed Loss (-) or Gain (+)	-4.38	0.0118	-3.7	-1.34	-1.29	-1.99
Hot Chimlet 1 (2012)	J2-619-IGT3	Calculated Conservative Mixture	7.07	0.0441	17.9	2.46	2.40	9.01
Hot Chimlet 1 (2012)	J2-619-IGT3	Observed Loss (-) or Gain (+)	-5.01	0.0124	-4.1	-1.66	-1.99	-2.20
Hot Chimlet 1 (2013)	N59-IGT6	Calculated Conservative Mixture	4.08	0.0254	22.2	2.46	1.39	9.51
Hot Chimlet 1 (2013)	N59-IGT6	Observed Loss (-) or Gain (+)	-4.06	0.0142	-1.5	-0.99	-0.88	0.93
Hot Chimlet 1 (2013)	N59-IGT4	Calculated Conservative Mixture	0.78	0.00487	26.9	0.47	0.27	10.07
Hot Chimlet 1 (2013)	N59-IGT4	Observed Loss (-) or Gain (+)	-0.77	0.00491	-0.5	-0.38	-0.09	0.24
Hot Chimlet 2 (2012)	J2-620-IGT4	Calculated Conservative Mixture	2.62	0.0164	24.2	1.58	0.89	9.76
Hot Chimlet 2 (2012)	J2-620-IGT4	Observed Loss (-) or Gain (+)	-1.94	0.0054	0.0	-0.55	-0.74	-0.41
Hot Chimlet 2 (2012)	J2-620-IGT8	Calculated Conservative Mixture	1.72	0.0107	25.5	1.04	0.59	9.91
Hot Chimlet 2 (2012)	J2-620-IGT8	Observed Loss (-) or Gain (+)	-1.21	0.0049	-2.4	-0.08	-0.43	-0.16
Hot Chimlet 3 (2013)	N62-IGT7	Calculated Conservative Mixture	6.43	0.0401	18.8	3.88	2.18	9.12
Hot Chimlet 3 (2013)	N62-IGT7	Observed Loss (-) or Gain (+)	-5.98	0.0242	-2.2	-1.85	-1.83	1.11
Hot Chimlet 3 (2013)	N62-IGT8	Calculated Conservative Mixture	1.99	0.0124	25.1	1.20	0.68	9.87
Hot Chimlet 3 (2013)	N62-IGT8	Observed Loss (-) or Gain (+)	-1.87	0.0105	-0.4	-0.75	0.35	0.45
Shrimp Gulley 1 (2012)	J2-620-IGT1	Calculated Conservative Mixture	3.73	0.0233	22.7	2.25	1.27	9.57
Shrimp Gulley 1 (2012)	J2-620-IGT1	Observed Loss (-) or Gain (+)	-3.33	0.0007	-0.1	-0.30	0.62	0.10
Shrimp Gulley 1 (2012)	J2-620-IGT2	Calculated Conservative Mixture	2.84	0.0177	23.9	1.71	0.96	9.72
Shrimp Gulley 1 (2012)	J2-620-IGT2	Observed Loss (-) or Gain (+)	-2.56	0.0028	-1.2	-0.59	0.62	0.33
Shrimp Gulley 2 (2012)	J2-618-IGT1	Calculated Conservative Mixture	1.89	0.0118	25.3	1.13	0.64	9.88
Shrimp Gulley 2 (2012)	J2-618-IGT1	Observed Loss (-) or Gain (+)	-1.77	-0.0010	0.1	-0.31	-0.55	0.32
Shrimp Gulley 2 (2012)	J2-618-IGT3	Calculated Conservative Mixture	1.32	0.0082	26.1	0.79	0.45	9.98
Shrimp Gulley 2 (2012)	J2-618-IGT3	Observed Loss (-) or Gain (+)	-1.35	0.0027	-0.9	0.04	-0.34	0.10
Shrimp Gulley 3 (2013)	N63-IGT6	Calculated Conservative Mixture	1.70	0.0106	25.6	1.02	0.58	9.91
Shrimp Gulley 3 (2013)	N63-IGT6	Observed Loss (-) or Gain (+)	-1.70	0.0093	-1.0	-0.52	1.98	0.19

^aJason (J2) or Nereus (N##) dive number and isobaric gas-tight sampler number (-IGT).

Table S4. Measured metal concentrations in the 'dissolved' fraction of Piccard fluids.

Vent (Year)	Sample	Al μm^3	Fe μm	Mn μm	Zn μm	Cu μm	Pb μm	Cd μm	Ag μm	Co μm
Hot Chimlet 1 (2012)	J2-619-IGT6	1.3	122	241	0.17	<0.11	<0.080	<0.089	<0.093	<0.17
Hot Chimlet 1 (2012)	J2-619-IGT3	3.3	100	268	<0.10	<0.11	<0.080	<0.089	<0.093	<0.17
Hot Chimlet 1 (2013)	N59-IGT6	<0.37	75	121	8.8	0.93	<0.080	<0.089	<0.093	<0.17
Hot Chimlet 1 (2013)	N59-IGT4	<0.37	13	29	3.3	0.40	<0.080	<0.089	<0.093	<0.17
Hot Chimlet 3 (2013)	N62-IGT8	<0.37	1032	75	4.0	8.1	0.78	<0.089	<0.093	<0.17
Hot Chimlet 3 (2013)	N62-IGT7	2.4	36	197	2.7	0.26	<0.080	<0.089	<0.093	<0.17
Hot Chimlet 2 (2012)	J2-620-IGT4	1.9	42	96	<0.10	<0.11	<0.080	<0.089	<0.093	<0.17
Hot Chimlet 2 (2012)	J2-620-IGT8	0.39	31	65	0.29	<0.11	<0.080	<0.089	<0.093	<0.17
Shrimp Gulley 1 (2012)	J2-620-IGT1	0.46	40	101	1.0	<0.11	<0.080	<0.089	<0.093	<0.17
Shrimp Gulley 1 (2012)	J2-620-IGT2	<0.37	52	88	0.11	<0.11	<0.080	<0.089	<0.093	<0.17
Shrimp Gulley 3 (2013)	N63-IGT6	<0.37	388	65	11	8.3	0.43	<0.089	<0.093	<0.17
Shrimp Gulley 2 (2012)	J2-618-IGT1	<0.37	26	44	0.16	<0.11	<0.080	<0.089	<0.093	<0.17
Shrimp Gulley 2 (2012)	J2-618-IGT3	3.4	24	43	1.9	<0.11	<0.080	<0.089	<0.093	<0.17

^amm, mmol/kg; μm , $\mu\text{mol/kg}$

Table S5. Measured metal concentrations in the 'filter' fraction of Piccard fluids.

Vent (Year)	Sample	Al μm^{a}	Fe μm	Mn μm	Zn μm	Cu μm	Pb μm	Cd μm	Ag μm	Co μm
Hot Chimlet 1 (2012)	J2-619-IGT6	0.14	14	1.1	0.10	0.88	<0.080	<0.0010	<0.0010	<0.0017
Hot Chimlet 1 (2012)	J2-619-IGT3	0.46	46	2.0	0.047	0.38	<0.080	<0.0010	<0.0010	<0.0017
Hot Chimlet 1 (2013)	N59-IGT6	– ^b	–	–	–	–	–	–	–	–
Hot Chimlet 1 (2013)	N59-IGT4	–	–	–	–	–	–	–	–	–
Hot Chimlet 3 (2013)	N62-IGT8	–	–	–	–	–	–	–	–	–
Hot Chimlet 3 (2013)	N62-IGT7	–	–	–	–	–	–	–	–	–
Hot Chimlet 2 (2012)	J2-620-IGT4	0.019	7.4	0.35	0.13	0.55	<0.080	<0.0010	<0.0010	0.0025
Hot Chimlet 2 (2012)	J2-620-IGT8	<0.010	3.7	0.16	0.048	<0.011	<0.080	<0.0010	<0.0010	<0.0017
Shrimp Gulley 1 (2012)	J2-620-IGT1	0.034	36	1.0	0.45	0.58	<0.080	<0.0010	<0.0010	0.0063
Shrimp Gulley 1 (2012)	J2-620-IGT2	<0.010	2.6	0.70	0.10	<0.011	<0.080	<0.0010	<0.0010	0.0023
Shrimp Gulley 3 (2013)	N63-IGT6	–	–	–	–	–	–	–	–	–
Shrimp Gulley 2 (2012)	J2-618-IGT1	<0.010	3.3	0.20	0.030	0.28	<0.080	<0.0010	<0.0010	0.0029
Shrimp Gulley 2 (2012)	J2-618-IGT3	<0.010	0.5	0.56	0.17	0.72	<0.080	<0.0010	0.0041	<0.0017

^amm, mmol/kg; μm , $\mu\text{mol/kg}$ ^b– not measured

Table S6. Measured metal concentrations in the 'dregs' fraction of Piccard fluids.

Vent (Year)	Sample	Al μm^{a}	Fe μm	Mn μm	Zn μm	Cu μm	Pb μm	Cd μm	Ag μm	Co μm
Hot Chimlet 1 (2012)	J2-619-IGT6	3.54	719	2.2	1.1	14	0.11	0.0035	0.059	0.27
Hot Chimlet 1 (2012)	J2-619-IGT3	– ^b	–	–	–	–	–	–	–	–
Hot Chimlet 1 (2013)	N59-IGT6	3.48	426	4.1	3.5	8.1	0.36	0.0045	<0.018	0.049
Hot Chimlet 1 (2013)	N59-IGT4	2.14	162	2.0	1.6	8.3	0.48	0.0030	<0.018	0.018
Hot Chimlet 3 (2013)	N62-IGT8	–	–	–	–	–	–	–	–	–
Hot Chimlet 3 (2013)	N62-IGT7	1.36	310	1.9	3.5	5.8	0.27	0.0052	<0.018	0.034
Hot Chimlet 2 (2012)	J2-620-IGT4	1.86	97.6	0.57	2.2	21	0.17	0.0046	0.097	0.098
Hot Chimlet 2 (2012)	J2-620-IGT8	3.93	126	0.90	2.1	14	0.10	0.0030	0.046	0.17
Shrimp Gulley 1 (2012)	J2-620-IGT1	7.88	1815	12	3.7	21	0.30	0.0075	0.102	0.18
Shrimp Gulley 1 (2012)	J2-620-IGT2	1.92	1529	2.0	5.1	208	0.12	0.0097	0.038	2.9
Shrimp Gulley 3 (2013)	N63-IGT6	0.174	2168	13	6.7	68	1.0	0.0082	<0.018	0.051
Shrimp Gulley 2 (2012)	J2-618-IGT1	0.923	62.3	0.46	1.1	7.5	0.077	0.0013	0.022	0.11
Shrimp Gulley 2 (2012)	J2-618-IGT3	1.32	88.7	0.61	4.2	39	0.49	0.011	0.052	<0.0017

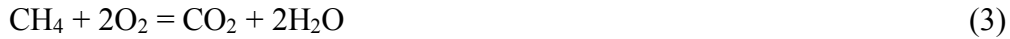
^amm, mmol/kg; μm , $\mu\text{mol/kg}$ ^b–' not measured

Thermodynamic Modelling

Two geochemical reaction path models were used to assess the impact of abiotic and thermogenic reactions during mixing on the amount of chemical energy available to support microbial metabolisms. Both models involved incremental mixing of a hydrothermal fluid with 2°C seawater over a temperature range of 160 to 5°C at 500 bar pressure. The initial temperature of 160°C represents the temperature calculated for the formation of the Hot Chimlet 1 fluid based on its measured Mg concentration by the mixing of the 398°C endmember Beebe Vent fluid with 2°C seawater, assuming that the heat capacity of the fluids remains constant with temperature. The lower measured temperature of 149°C at Hot Chimlet 1 likely reflects technical challenges associated with placing the temperature probe in the region of hottest flow during seafloor measurement. For the first model, the starting composition of the hydrothermal fluid represents a conservative mixture of the endmember Beebe Vent fluid with anaerobic seawater to achieve a Mg concentration identical to the Hot Chimlet 1 fluid. For the second model, the composition of the fluid in 2012 (J2-619-IGT6, Table 1) was used for the starting composition of the hydrothermal fluid. At each step during the incremental mixing of hydrothermal fluid and seawater, the equilibrium distribution of aqueous species was calculated for that temperature using Version 8.0a of the EQ3/6 computer program (2) and a thermodynamic database generated at 500 bar using SUPCRT92 (3), as compiled in Klein and Bach (4) and Klein et al (5). The modeling approach is similar to that used previously to study the distribution of energy types in seafloor hydrothermal systems (6, 7). Redox equilibrium was suppressed for all species, including O₂ and H₂, and those that contain C, S, and Fe. These assumptions are based on the observation of slow reaction kinetics at moderate temperatures for the equilibration of sulfate-sulfide (8), inorganic carbon-methane (9), and H₂-O₂ (10). The precipitation of all minerals was suppressed. It was assumed that fully oxidized seawater containing 0.2 mmol/kg O₂ (11) and the measured composition in Table 1 was available to mix with hydrothermal fluids at all temperatures. Activity coefficients for the neutrally charged aqueous gases H₂, CH₄, O₂ were assumed to be equal to 1, while other activity coefficients were set by the EQ3/6 model output.

Model results were used to calculate the maximum amount of potential chemical energy available to support five chemolithoautotrophic metabolic pathways: sulfate reduction, methanogenesis, methanotrophy, sulfide oxidation, and hydrogen oxidation, according to the reactions:





The amount of metabolic energy that is potentially available to a microorganism carrying out a particular metabolic reaction is calculated using the equation:

$$\Delta G = \Delta G^\circ + RT \ln Q \quad (5)$$

Where ΔG° symbolizes the standard free energy of reaction, ΔG the free energy of reaction, R the universal gas constant, T the temperature in Kelvin, and Q the activity product of the reactant and product species. In order to describe the available energy in joules per kilogram of mixed fluid, the calculated ΔG value for each model step was multiplied by the concentration of the compound that would be limiting, scaled to reaction stoichiometry (6, 7). The stoichiometric scaling factor is the same in both scenarios, as is the O_2 concentration at each mixing step, but the H_2 concentration differs on account of the different starting compositions. For reactions 1 and 2, the limiting reactant is assumed to be H_2 , while for reactions 2-4 the limiting reactant is assumed to be O_2 . For reaction 5, the limiting reactant is O_2 at higher temperatures when H_2 is relatively more abundant. This limiting reactant then switches to H_2 at lower temperatures as O_2 increases in relative availability. This switch from limiting O_2 to limiting H_2 occurred at a temperature of 13°C and 31°C, for scenarios 1 and 2, respectively. At each mixing increment at temperatures less than or equal to 122°C, the percent difference between the potential energy available in the actual Hot Chimlet 1 (2012) fluid and that in the theoretical fluid was calculated for reactions 1-5. This approach determines the impact of H_2 and SO_4 losses and CH_4 gains on energy availability in a natural system that is impacted by abiotic and thermogenic reactions occurring at moderate temperatures above the limit for life, but well below source fluid temperatures. Energy availability in the actual fluid is then compared to what might otherwise be expected based on conservative mixtures that model theoretical mixed fluid chemistries by starting with the composition of a 350-400°C source fluid.

Table S7. Composition of theoretical starting composition of hydrothermal fluid in scenario 1.

T	(°C)	160
pH	(160°C, 500 bar)	7.15
O ₂ , aq	(mmol/kg)	0
H ₂ , aq	(mmol/kg)	1.95
SO ₄ ²⁻	(mmol/kg)	18.9
ΣH ₂ S	(mmol/kg)	3.81
Na ⁺	(mmol/kg)	419
Ca ²⁺	(mmol/kg)	9.14
Mg ²⁺	(mmol/kg)	35.4
Al ³⁺	(mmol/kg)	0.00500
Fe ²⁺	(mmol/kg)	2.14
Cl ⁻	(mmol/kg)	484
ΣCO ₂	(mmol/kg)	9.09
CH ₄	(mmol/kg)	0.0394
SiO ₂ , aq	(mmol/kg)	5.80
K ⁺	(mmol/kg)	10.3
Mn ²⁺	(mmol/kg)	0.244

SUPPLEMENTARY INFORMATION REFERENCES

1. J. S. Seewald, *et al.*, Submarine venting of magmatic volatiles in the Eastern Manus Basin, Papua New Guinea. *Geochim. Cosmochim. Acta* **163**, 178–199 (2015).
2. T. J. Wolery, “EQ3NR, a computer program for geochemical aqueous speciation-solubility calculations: Theoretical manual, user’s guide, and related documentation” (1992)
<https://doi.org/10.2172/138643>.
3. J. W. Johnson, E. H. Oelkers, H. C. Helgeson, SUPCRT92: A software package for calculating the standard molal thermodynamic properties of minerals, gases, aqueous species, and reactions from 1 to 5000 bar and 0 to 1000°C. *Comput. Geosci.* **18**, 899–947 (1992).
4. F. Klein, W. Bach, Fe-Ni-Co-O-S Phase Relations in Peridotite-Seawater Interactions. *J. Petrol.* **50**, 37–59 (2009).
5. F. Klein, W. Bach, T. M. McCollom, Compositional controls on hydrogen generation during serpentinization of ultramafic rocks. *Lithos* **178**, 55–69 (2013).
6. T. M. McCollom, E. L. Shock, Geochemical constraints on chemolithoautotrophic metabolism by microorganisms in seafloor hydrothermal systems. *Geochim. Cosmochim. Acta* **61**, 4375–4391 (1997).

7. T. M. McCollom, Geochemical constraints on sources of metabolic energy for chemolithoautotrophy in ultramafic-hosted deep-sea hydrothermal systems. *Astrobiology* **7**, 933–950 (2007).
8. H. Ohmoto, A. C. Lasaga, Kinetics of reactions between aqueous sulfates and sulfides in hydrothermal systems. *Geochim. Cosmochim. Acta* **46**, 1727–1745 (1982).
9. T. M. McCollom, Abiotic methane formation during experimental serpentinization of olivine. *Proc. Natl. Acad. Sci.* **113**, 13965–13970 (2016).
10. D. I. Foustoukos, J. L. Houghton, W. E. Seyfried, S. M. Sievert, G. D. Cody, Kinetics of H₂–O₂–H₂O redox equilibria and formation of metastable H₂O₂ under low temperature hydrothermal conditions. *Geochim. Cosmochim. Acta* **75**, 1594–1607 (2011).
11. T. M. Joyce, A. Hernandez-Guerra, M. Smethie Jr., Zonal circulation in the NW Atlantic and Caribbean from a meridional World Ocean Circulation Experiment hydrographic section at 66°W. **106**, 22095–22113 (2001).